Spreading Resistance of a Contact Spot on a Thin Film

Peng Zhang[1], Y. Y. Lau[1] and Roland S. Timsit[2]
[1]Department of Nuclear Engineering and Radiological Sciences, University of Michigan, Ann Arbor, MI, USA 48109-210
[2]Timron Scientific Consulting, Inc.,Toronto, ON M5M1L6, Canada

Abstract—**Thin film contacts are becoming increasingly important in the miniaturization of electronic devices. This paper considers the spreading resistance of a microscopic contact of size *a* ("*a*-spot") on a thin film. The effect of the film thickness *h* on the spreading resistance is evaluated over a large range of the aspect ratio *a*/*h*, for both Cartesian and cylindrical geometries. In the limit $h \rightarrow 0$, the normalized spreading resistance converges to finite values. An interpretation of these limits is given, along with the implication of intense local heating at the rim of the *a*-spot. The analytic theory is extended to *a*-spots of arbitrary shape; and is applicable to AC bulk contact resistance calculations at sufficiently high excitation frequencies. Results of the analytic theory are compared with recent measurements and simulations of contact resistance in cylindrically symmetric contacts. Because existing models are generally valid over different ranges of contact radius and film thickness, even for an idealized geometry, this paper emphasizes the importance of comparing measured spreading resistance with values calculated from the model that is applicable to the experimental situation.**

Keywords— electrical contacts; thin films; current crowding; constriction resistance; contact resistance, spreading resistance; skin depth

I. INTRODUCTION

Thin film contacts are becoming increasingly important in the miniaturization of electronic devices such as micro-electromechanical system (MEMS) relays and microconnector systems, where thin metal films of a few microns are typically used to form electrical contacts. Thin film contacts are also important in integrated circuits [1], and in materials and device characterization [2].

In this paper, we focus only on the thin film geometry shown in Fig. 1, which we shall label either as a Cartesian (rectangular symmetry) film or as a cylindrical film. The thin film is characterized by a thickness h and an electrical resistivity ρ. A voltage V_0 is applied uniformly along the edge of the Cartesian (cylindrical) thin film, at $y = \pm b$ ($r = b$). A grounded electrode is attached to the top region, AB, where the B-coordinates are $y = \pm a$ ($r = a$) in the Cartesian (cylindrical) geometry. Following Holm, we shall identify the terminal AB as the single "a-spot" [3-5]. As we shall see, the accurate numerical evaluation [6,7] of the electrical resistance to current flowing through the a-spot and spreading through the thin film, for the Cartesian and the circular configurations, allows ready extension of the theory to a general a-spot geometry in the limit $h \rightarrow 0$ [7,8]. This calculation of the DC

This work was supported by an AFOSR grant on the Basic Physics of Distributed Plasma Discharge, AFOSR grant FA9550-09-1-0662, and L-3 Communications Electron Devices Division.

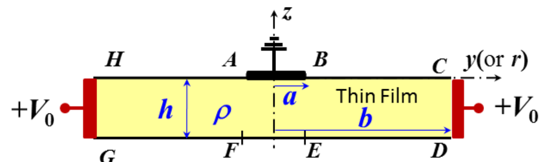

Fig. 1. Cartesian (2D cross-sectional view) and cylindrical thin film. In the cylindrical geometry, the vertical axis at the center is the axis of rotation.

spreading resistance may also be applied to the high-frequency AC current in a bulk solid [9,10] where the current flow is limited to the skin depth, δ, by letting $h = \delta$. We also aim to show that our exact calculation of the spreading resistance for the contact geometry of Fig. 1 yields insights for the proper interpretation of experimental measurements of constriction resistance [11-13].

The paper is structured as follows. Section II summarizes useful theoretical results for spreading resistance and current flow for the thin film geometry of Fig. 1, from previous work. The calculations were based on an exact theory formulated for arbitrary values of a, b, and h, for both Cartesian and cylindrical geometries [6,7]. In Section III, we extend the theory to an a-spot of a general geometry [7,8]. In Section IV, we apply the DC thin film theory to the AC bulk contact [8]. Section V compares the evaluation of spreading resistance from our exact theory with evaluations from recent computer simulations and with results from recent experimental measurements [13].

II. SPREADING RESISTANCE AND CURRENT FLOW IN A THIN FILM

In Fig. 1, the current flow is orthogonal to the electrodes AB, CD and GH, and becomes parallel to the thin film boundary GD, BC and HA after spreading for a sufficient distance from AB. The total resistance, R_T, between the terminals AB and CD (and GH) may be expressed in terms of the bulk resistance, R_{bulk}, and the spreading resistance, R_s. Because the current flow lines do not curve sharply and become parallel to the thin film surface exactly at $y = a$, (or $r = a$), there is arbitrariness in the definitions of R_s and R_{bulk} but this arbitrariness is restricted by the condition that the *total* resistance $R_T = R_s + R_{bulk}$ remains the same for selected thin-film dimensions and a selected contact geometry [8].

978-1-4673-5281-9/13/$31.00 ©2013 IEEE

Regardless of how R_{bulk} is defined, the thin film spreading resistance (constriction resistance) R_s is, in general,

$$R_s = R_T - R_{\text{bulk}}. \quad (1)$$

For Fig. 1, we find it convenient to *define* R_{bulk} to be the bulk resistance from BE to CD and from AF to GH, yielding [8],

$$R_{bulk} = \rho(b-a)/2hW, \text{ [Cartesian]} \quad (2a)$$

$$R_{bulk} = (\rho/2\pi h)\,\ell n(b/a), \text{ [cylindrical]} \quad (2b)$$

for the Cartesian and cylindrical geometry, respectively, where W in the Cartesian geometry denotes the channel length in the direction perpendicular to the paper. A different definition of R_{bulk} would lead to a different expression of the spreading resistance R_s.

Next we normalize the spreading resistance to $\overline{R}_s$ as follows

$$R_s = \frac{\rho}{4\pi W}\overline{R}_s, \quad \text{[Cartesian]} \quad (3a)$$

$$R_s = \frac{\rho}{4a}\overline{R}_s, \quad \text{[cylindrical]} \quad (3b)$$

where the normalized resistance depends only on the aspect ratios a/h and a/b, in accordance with the solution of the Laplace equation corresponding to the system in Fig.1. Furthermore, if either $b >> a$, *or* $b >> h$, the current flow at terminals CD and GH is uniform, and both R_s and $\overline{R}_s$ are independent of b. Previous work [12] and our own previous calculations [6-8] have shown that the normalized resistance can be expressed as

$$\overline{R}_s = 2\pi\frac{a}{h} - 4\ln\left[\sinh\left(\frac{\pi}{2}\frac{a}{h}\right)\right], \quad \text{[Cartesian]} \quad (4a)$$

$$\overline{R}_s = \begin{cases} 1 - 2.2968(a/h) + 4.9412(a/h)^2 - 6.1773(a/h)^3 \\ +3.811(a/h)^4 - 0.8836(a/h)^5, \quad 0 \le a/h \le 1; \\ 0.28 + 0.0502(h/a) + 0.0523(h/a)^2, \ 1 < a/h < \infty. \end{cases} \quad \text{[cylindrical]} \quad (4b)$$

Equation (4a) is the exact expression for the Cartesian thin film in the asymptotic limit $b >> a$, *or* $b >> h$ [12]. Equation (4b) was synthesized both from the data generated from an analytical solution of the boundary value problem describing current flow in the contact assembly of Fig. 1, [7,8] and from MAXWELL 2D simulations [14] of the cylindrical thin film in the limit $b >> a$, *or* $b >> h$. The variations of the normalized spreading resistance with a/h evaluated from Eqs. (4a) and (4b) are shown by the solid curves in Figs. 2 and 3 respectively [6-8]. Note that as $a/h \to \infty$, $\overline{R}_s$ approaches the asymptotic limit of $4\ell n2 = 2.77$ and $4\ell n2/\pi^2 = 0.28$, respectively in Figs. 2 and 3 [8]. As $a/h \to 0$, $\overline{R}_s \to -4\ell n(a/h)$ according to Eq. (4a), and $\overline{R}_s \to 1$ according to Eq. (4b). These limits are consistent with the requirement that R_s defined respectively in Eqs. (3a) and (3b) must tend to infinity as $a \to 0$.

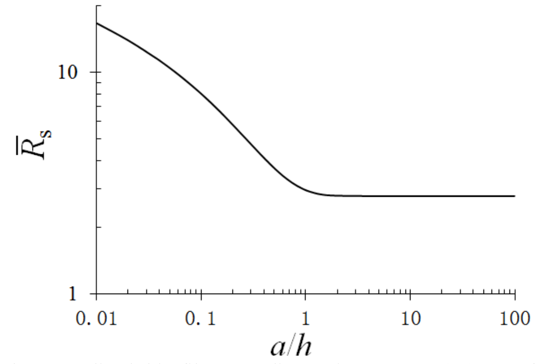

Fig. 2. The normalized thin film spreading resistance, Eq. (4a), as a function of a/h, for the Cartesian structure in Fig. 1.

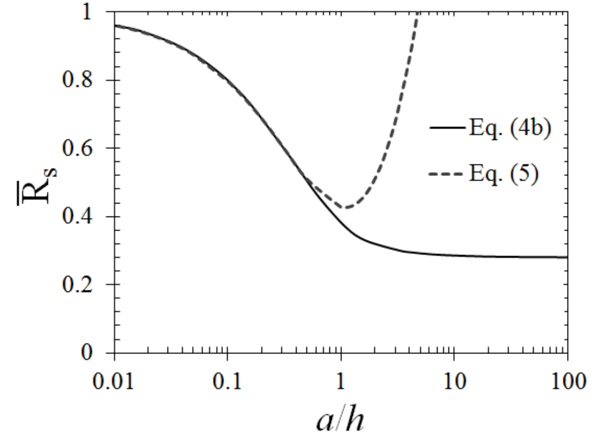

Fig. 3. The normalized thin film spreading resistance, Eq. (4b), as a function of a/h, for the cylindrical structure in Fig. 1. The dashed line shows Timsit's approximate formula, Eq. (5), which is valid for $a/h < 0.5$.

In an analytical approach to the calculation of spreading resistance, and by approximating the current density distribution through the circular a-spot with the known current density distribution through the a-spot in a semi-infinite bulk solid [4], Timsit obtained the following expression for $\overline{R}_s$ for $0 < a/h < 0.5$, [9]

$$\overline{R}_s = \frac{4}{\pi}\sum_{n=1}^{\infty}\coth\left(\frac{\lambda_n h}{b}\right)\frac{\sin\left(\frac{\lambda_n a}{b}\right)}{J_1^2(\lambda_n)\lambda_n^2} - \frac{2a}{\pi h}\ln\left(\frac{b}{a}\right), \quad 0 < \frac{a}{h} \le 0.5. \quad (5)$$

Because of the approximation of the current density distribution, Timsit [9] emphasized that Eq. (5) is not expected to be valid for $a/h > 0.5$. This prediction of Timsit is confirmed by the dashed curve in Fig. 3, which shows that Eq. (5) is an excellent approximation to $\overline{R}_s$ if, and only if, $a/h < 0.5$ [7,8].

The electrical current streamlines in the right half of the thin film structure of Fig. 1 are shown in Fig. 4, for the Cartesian thin film, with a/h = 10 and b/a = 8. The current streamlines for the cylindrical thin film are indistinguishable from those in Fig. 4 for identical values of a/h and b/a [8]. The streamlines in both the Cartesian and the cylindrical thin film were calculated from a series expansion method, and were validated by conformal mapping method for the Cartesian thin film [7]. The physical reason for the essentially identical flow patterns in the Cartesian and the cylindrical films, if $h << a$, is as follows. Once a is fixed, in the limit $h \rightarrow 0$, the current streamlines spread over such an infinitesimal thickness h that the shape of the edge "B" in Fig. 1 (whether Cartesian or cylindrical geometry), no longer affects significantly the current streamlines near the a-spot boundary.

We have shown that, for both Cartesian and cylindrical thin films, the current spreads from the a-spot into the film within a length scale L_T from the rim (point B) of the a-spot (Fig. 4), where this current "transfer length" is given by [8],

$$L_T = (2/\pi)\ell n 2 \times h = 0.44h, \qquad h << a \qquad \text{[Cartesian and cylindrical]} \qquad (6)$$

An interpretation of L_T is that, in the limit of $h \rightarrow 0$, the bulk resistance between $r = a - L_T$ and $r = b$, for the cylindrical thin film, is equal to the total thin film resistance R_T. If one adopts such a definition for the bulk resistance R_{bulk}, the spreading resistance R_s then goes to zero as $h \rightarrow 0$. A similar interpretation applies to (the same) L_T for the Cartesian thin film. This is an illustration of the arbitrariness in the definition of R_{bulk}, and therefore in the spreading resistance R_s; only R_T remains the same in Eq. (1) [8], for a given set of values of a, b, h, and ρ in Fig. 1.

Figure 4 shows intense current crowding at the edge B of the a-spot in Fig. 1, leading to localized Joule heating at the rim of the a-spot if $h << a$. Such localized enhanced heating has been observed in bulk electrical contacts [15], but its contribution to contact overheating may be greatly magnified in a thin film contact since heat is less effectively dissipated in a thin film contact.

III. Extension to A-spot of General Geometry

Since the transfer length, L_T in Eq. (6), and the current flow patterns shown in Fig. 4 are the same for both Cartesian and cylindrical thin films in the $h \rightarrow 0$ limit, we may extend the theory to a general a-spot as illustrated in Fig. 5. We propose that, for the a-spot shape shown in Fig. 5, the spreading resistance R_s defined in Eq. (1) would assume the general form [7,8],

$$R_s = \left(\frac{\rho}{L}\right)\frac{2\ell n 2}{\pi}, \quad h \rightarrow 0, \qquad (7)$$

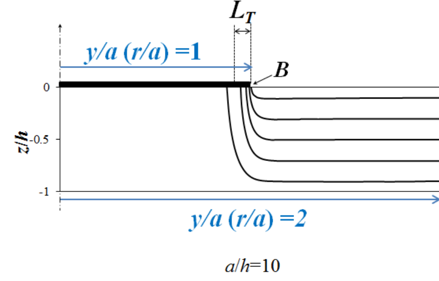

Fig. 4.The current streamlines in the right half of the Cartesian thin film in Fig. 1 are calculated from both series expansion method [cf., Eq. (A8) of Ref. [6]] and conformal mapping, for the case of a/h = 10. The current streamlines calculated for the cylindrical thin film of Fig. 1 are indistinguishable from those in the Cartesian case [8].

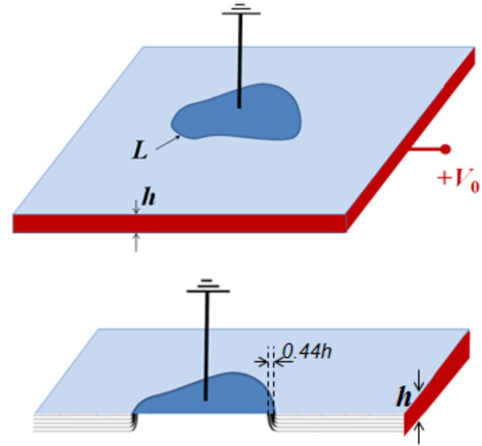

Fig. 5. a-spot of an arbitrary shape. Note that the current streamlines in the bottom figure are identical to Fig. 4 locally.

where L is the circumference of the a-spot of an arbitrary shape, and R_{bulk} is the bulk resistance of the thin film exterior to this generalized a-spot. For a circular a-spot of radius a, $L = 2\pi a$, and Eq. (7) gives $R_s = 0.28 \times (\rho / 4a)$ which is consistent with Fig. 3 in the limit $h \rightarrow 0$. For an a-spot in the Cartesian geometry, $L = 2W$ (the factor of two to account for both edges A and B in Fig. 1), and Eq. (7) gives $R_s = 2.77 \times (\rho / 4\pi W)$ which is consistent with Fig. 2 in the limit $h \rightarrow 0$. Clearly, there will be limitations to the validity of Eq. (7), particularly if the a-spot shape is highly irregular e.g. where the radius of curvature s of the a-spot varies significantly in magnitude and sign along the circumference. For a-spots with relatively smooth boundaries (Fig. 5), we propose that Eq. (7) provides a valid description of spreading resistance for a single a-spot of arbitrary shape if $h <<$ minimum s.

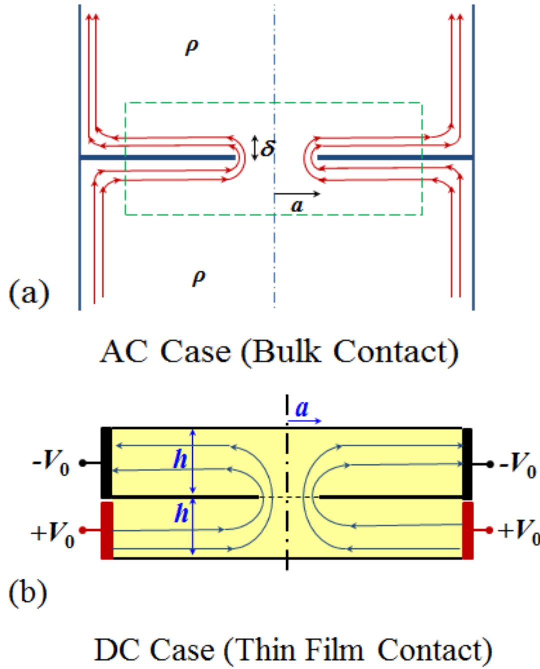

Fig. 6 (a) High-frequency AC current in a bulk solid with constriction of size a where the current flow is limited to the skin depth δ [9], and (b) The DC thin film contact. Due to symmetry, the potential profile and constriction resistance in the bottom half of the thin film are identical to those of Fig. 1.

IV. Extension to AC Bulk Contact

Timsit [9] pointed out that DC current spreading from a constriction in a thin film is reminiscent of the spreading pattern at high frequencies through a constriction in a bulk solid where current flow is limited to the skin depth, δ (Fig. 6a). The similarities between the DC current flow in a thin film and current flow at high frequencies led to the speculation that AC current flow through the penetration depth δ is equivalent to DC flow in a thin film of thickness h, where h would be identified as δ, as indicated in Fig. 6b [9,10]. If such an equivalence holds, then it would be possible to calculate constriction resistance at high frequencies in a bulk solid from the DC spreading resistance properties in a thin film. We now consider the possibility of such an equivalence.

If we assume that the equivalence holds, and h is identified with δ, then the calculated limits of $\overline{R}_s$ = 2.77 for the Cartesian case and $\overline{R}_s$ = 0.28 for the cylindrical case as $h \rightarrow 0$ should apply to the AC case as the skin depth $\delta \rightarrow 0$. The dashed curve in Fig. 7 represents the variation with increasing a-spot diameter of the DC thin film constriction resistance evaluated from $R_s = (\rho/4a)\overline{R}_s = 0.28 \times (\rho/4a)$. In these evaluations, we have used the asymptotic value of $\overline{R}_s$ = 0.28 as $a/h \rightarrow \infty$ [cf. Eq. (4b)]. Figure 7 also shows calculated variations of AC constriction resistance with increasing constriction diameter for various frequencies reported earlier [9,10] for the cylindrical contact geometry of Fig. 6a. One of the major observations in this earlier work was that, for a selected constriction diameter, constriction resistance decreases with increasing excitation frequency. In other words, AC constriction resistance decreases as $\delta \rightarrow 0$, which is also the pattern observed with thin film DC resistance as $h \rightarrow 0$ as shown in Figs. 2 and 3. The important feature in Fig. 7 is that the dashed curve is closest to the lowest solid curve in Fig. 7 that corresponds to the constriction resistance at the highest frequency (1 GHz) and hence at the smallest skin depth δ in that plot. Furthermore, we verified that the 1GHz curve in Fig. 7 is essentially identical with the curve described from R_s = 0.3 ($\rho/4a$). The striking observation in Fig. 7 is that the normalized resistance of 0.3 for the 1 GHz curve is very close to the limiting value of 0.28 mentioned above for normalized constriction resistance for the DC thin film [7,8]. This observation appears to support the case for an equivalence between properties of spreading resistance at high frequencies and DC spreading resistance in a thin film of thickness δ. On the basis of this observation, there are grounds for suggesting that the AC normalized resistance should

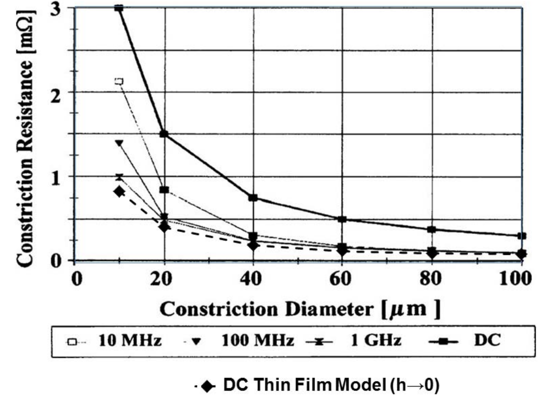

Fig. 7. The DC thin film model ($h \rightarrow 0$) as the limiting case for the high frequency AC bulk contact resistance [9], [10], once the skin depth δ for the AC bulk contact is identified with the thin film thickness h.

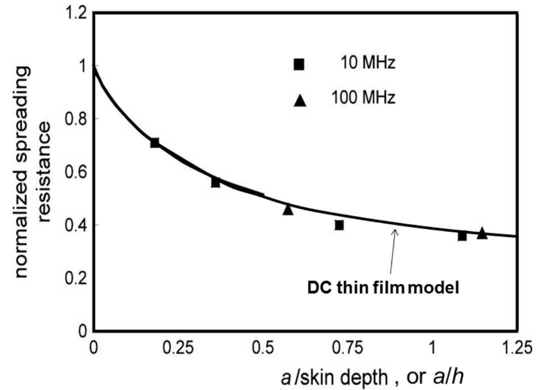

Fig. 8 Comparison of the variations of normalized spreading resistance versus a/h calculated on the basis of the DC thin film model studies in Sec II, with the values associated with AC bulk spreading resistance where h is replaced by the skin depth δ [9]. As $a/\delta \rightarrow \infty$, the curve is expected to converge to a final value of 0.28, as predicted by the DC thin film model [Eq.(4b) and Fig. 3].

decrease only to ~ 0.28 for very high frequencies since $\overline{R}_s$ = 0.28 for a/h >> 1 in Eq. (4b). Likewise, we conjecture that Fig. 10 of [9], which is reproduced in Fig. 8, would converge to the final value of ~ 0.28 as $a/\delta \to \infty$.

Figure 8 shows the variation of AC normalized resistance with decreasing δ (i.e. increasing a/δ). The data points are derived from the curves of Fig. 7. The solid curve is a plot of Eq. (4b) for the DC thin film case where the thickness h has been replaced by the skin depth δ. Clearly, Eq. (4b) provides an excellent description of the variation of normalized constriction resistance with decreasing skin depth (or increasing frequency). We propose that Eq. (4b) may be used to provide reliable estimates of AC constriction resistance in bulk contact over a wide range of excitation frequencies exceeding 1 GHz for the parameters of Fig. 7. We also propose that, on the basis of our conjecture in Section III, Eq. (4b) may be used to estimate AC constriction resistance of a constriction of irregular shape, such as illustrated in Fig. 5, for excitation frequencies beyond 1 GHz. Since the "DC thin film model" in Fig. 8 appears to yield the correct limits for both small and large skin depth, it is possible that Eq. (4b) may in fact be applicable from low to high frequencies, and this speculation [7] is to be subjected to future tests.

V. On the Measurement of Spreading Resistance

In this section, we address some intrinsic difficulties in experimental measurements of the contact (constriction) resistance. Typically, what is measured in a circuit (Fig. 1) is the total resistance, R_T, which is the ratio of the applied voltage V_0 between the terminals and the total current I in the circuit, $R_T = V_0/I$. The spreading resistance R_s in Fig. 1 is then obtained by subtracting the bulk resistance R_{bulk} from this measured total resistance R_T, i.e., $R_s = R_T - R_{bulk}$, as shown in Eq. (1). The accuracy of the extracted contact resistance R_s is thus critically dependent on the correct elimination of the bulk resistance R_{bulk} for the given circuit. There are challenges to the correct measurement of contact resistance in a thin film, as addressed below.

We recall that there is arbitrariness in the decomposition of the total resistance R_T into constriction resistance R_s and R_{bulk}, as discussed in Section II. A valid comparison between the results of experimental measurements and those of theory is possible only if a consistent definition of the bulk resistance is used throughout. One of the factors affecting bulk resistance is the location of electrodes on the thin film in an experimental setup, since this affects the current flow pattern in the thin film and hence affects the measured magnitude of both the total resistance and bulk resistance. For example, attachment of the current-collector electrode only *to a portion on the surface* MN of the thin film as illustrated schematically in Fig. 9(a) rather than to *the entire thin film rim* as illustrated in Fig. 9(b) for the cylindrical case greatly influences R_{bulk} and also complicates its evaluation. In these two examples of experimental layouts, the bulk resistance in the geometry of Fig. 9(a) is appreciably larger than that in Fig. 9(b) since current spreads through a narrower pathway. Since the constriction resistance is a small quantity obtained from the subtraction of two large numbers i.e. subtraction of the bulk resistance from the total resistance [cf. Eq. (1)], a large uncertainty in R_{bulk} may lead to a large uncertainty in the determination of R_s.

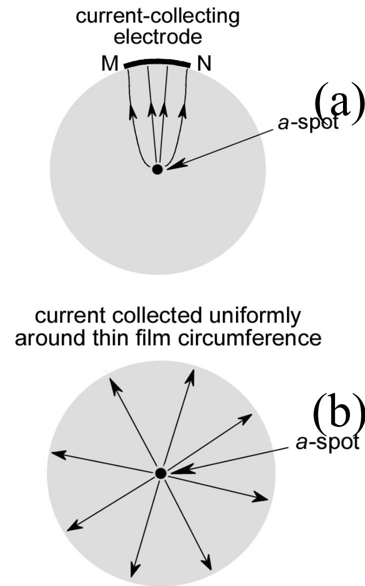

Fig. 9. Schematic drawing of current flow in a cylindrical thin film where the current is collected (a) over a segment MN of the circumference and (b) over the entire circumference of the thin film.

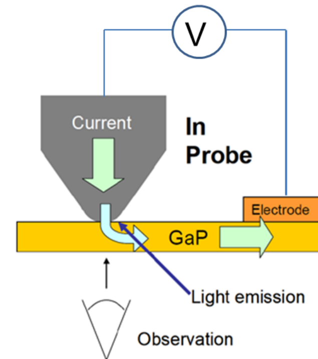

Fig. 10. Schematic drawing of experimental setup of Sawada *et al* [13].

There is an additional source of uncertainty in the measurements of spreading resistance that relates to the measurement technique. If the measurement is carried out using a two-terminal rather than the more conventional four-terminal approach, then a correction must be introduced to account for the unavoidable contact resistance at the measuring electrodes. Clearly, the difficulties for the correct evaluation of contact resistance R_s from voltage-drop and current measurements in a thin film represent a significant challenge.

There have been only a few serious attempts to measure contact resistance with a thin film using a contact geometry similar to that illustrated in Fig. 1 [11,13]. In their recent report of contact resistance measurements, Sawada *et al* [13] used a contact assembly consisting of a cylindrical rod pressing on a circular GaP thin film wafer. The contact assembly was similar to that shown in Fig. 1. This similarity provided an opportunity to compare the results of Sawada *et al*'s measurements with values of contact resistance calculated from Eq.(4b). On account of this comparison, we have reproduced the experimental setup described by Sawada *et al* [13] in Fig. 10. This setup appears to have relied on a two-terminal measurement approach wherein current was passed through the spherical contact end of the pin and collected by an electrode deposited on a part of the outer film circumference. The arrangement is similar to Fig. 9(a), and differs from that of other workers [11]. In the following paragraph, we review the experimental data presented in [13] and compare these data with predictions from our analytical model described in Section II. We also compare the results of contact resistance evaluations from our model with those from simulations also carried out by Sawada *et al* [13].

In the experimental arrangement in [13], the total resistance $R_{T,exp}$ between the spherical tip of the contact rod and the thin film electrode located at the wafer edge may be expressed as follows

$$R_{T,exp} = R_S + R_{Bulk,wafer} + R_{CE} \tag{8}$$

In the above expression, R_S is the contact (spreading) resistance to be determined, $R_{Bulk,wafer}$ is the bulk resistance between the *a*-spot and the collecting electrode as illustrated in Fig. 9(a), and R_{CE} is the contact resistance of the current-collector electrode with the wafer edge. We emphasize that R_{CE} is not necessarily zero even if the collecting electrode consists of a film deposited with complete metallurgical bonding with the wafer since the current must spread into this electrode and thus gives rise to a spreading resistance.

The comparison of Sawada *et al*'s experimental data with the predictions of Eq. (4b) is shown in Fig. 11. In this comparison, we recall that the experimental data were obtained from measurements of the total resistance $R_{T,exp}$ and the subsequent subtraction of the bulk resistance $R_{Bulk,wafer}$ in Eq. (8) [13]. The experimental data are shown as circles and triangles respectively for a 200 µm and a 50 µm film, and the solid and dashed lines show the corresponding curves calculated from theory. The data comparison in Fig. 11 points to a clear disagreement between the experimental data and the predictions of theory (Eq. (4b)). We now attempt to identify the sources of this disagreement.

The experimental data of Fig. 11 required an accurate evaluation of the bulk resistance $R_{Bulk,wafer}$ and the contact resistance R_{CE} of the current-collector electrode. The description in Sawada *et al* [13,16] of evaluations of $R_{T,exp}$ is ambiguous on how $R_{Bulk,wafer}$ can be reliably evaluated.

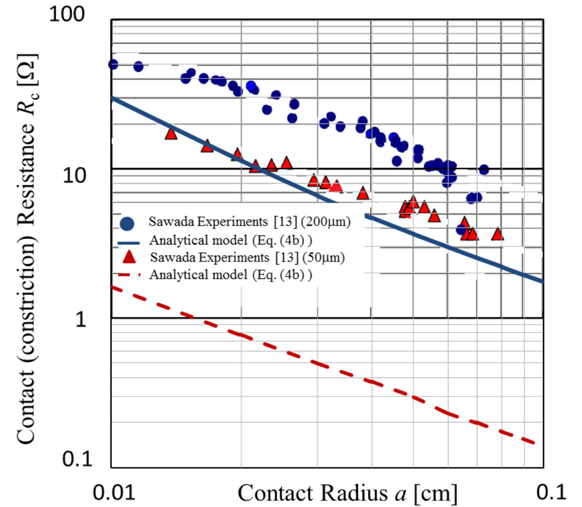

Fig. 11 Comparison of data calculated from the analytical model, Eq. (4b), with measured values from Sawada *et al*'s experiments (Fig. 14 of [13]). For the analytical model, the resistivity and dimensions are taken from [13]: for *h*=200µm, ρ = 2.3Ω-cm; for *h* = 50µm, ρ = 0.2Ω-cm. The radius of the thin film disk is *b* = 5mm.

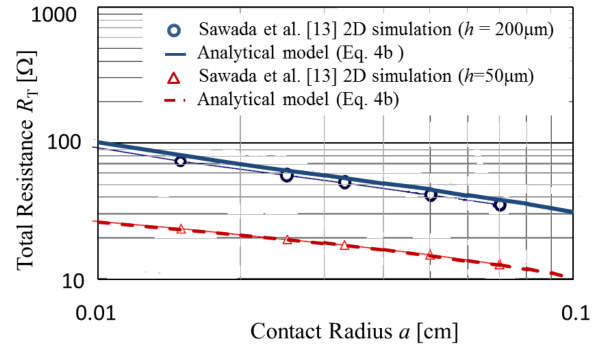

Fig. 12 Comparison of data calculated from the analytical model, Eq. (4b), with those from Sawada *et al*'s 2D simulation (Fig. 12 of [13]). For the analytical model, the resistivity and dimensions are taken from [13]: for *h*=200µm, ρ = 2.3Ω-cm; for *h* = 50µm, ρ = 0.2Ω-cm. The radius of the thin film disk is *b* = 5mm.

Because the resistivity of the GaP material used for the thin films was large, even a small error in $R_{Bulk,wafer}$ would have led to a large error in the evaluation of R_S. For example, if the current collector electrode covered the entire wafer rim, the bulk resistance would be given as Eq. (2b),

$$R_{Bulk,wafer} = R_{Bulk,circum} = \frac{\rho}{2\pi h}\ln\left(\frac{b}{a}\right)$$

where h and b are respectively the thickness and outer radius of the thin film wafer. If the angle subtended by the current-collector electrode used by Sawada *et al* [13] is denoted as φ, and if it is assumed that the current emanating from the *a*-spot was largely confined within the sector defined by φ, then the bulk resistance $R_{Bulk,wafer}$ would be larger than $R_{Bulk,circum}$ defined above by a factor of approximately $(360/\varphi)$, where φ

is in degree. We suggest that the large discrepancy between the experimental and theoretical data in Fig. 11 stems largely from the use of too small a value of the bulk resistance by Sawada *et al* in extracting the constriction resistance from Eq.(8). In addition, in that same paper, the measured total resistance values of $R_{T,exp}$ are compared with the expression

$$R = \frac{\rho}{\pi a}\sum_{n=1}^{n=\infty}\frac{\coth\left(\frac{\lambda_n h}{b}\right)\sin\left(\frac{\lambda_n a}{b}\right)}{\left(J_1(\lambda_n)\lambda_n\right)^2} \quad (9)$$

derived earlier by Timsit [9] under the assumption $a/h < 0.5$ [cf. Eq. (5)]. Equation (9) describes the approximate total resistance, including the spreading resistance and the bulk resistance, between the *a*-spot and the rim of a cylindrical thin film of outer radius b and thickness h (Fig. 1). A comparison of the measured total resistance with the above expression in [13] is questionable not only because Eq. (9) does not apply to the experimental contact layout but also because the formula was stated to be valid only for $a/h < 0.5$ in the original publication [9] (cf., Fig. 3) whereas a great deal of the data in [13] corresponded to cases where $a/h \geq 2$.

Other possible sources for the discrepancies between experimental and theoretical data in Fig. 11 include the neglect of contact resistance at the current-collector electrode and the presence of possible electrically insulating thin surface films on the wafer.

Sawada *et al* [13] also reported results of computer simulations of thin film contacts in order to compare with their experimental data. However, the geometry of the contact assembly used in some of these simulations corresponded to that of Fig. 1, rather than replicating the assembly used for their experimental measurements where the current-collector electrode was situated over only part of the cylindrical film circumference. Hence and as expected, the results of such 2D numerical analysis of contact resistance did not agree with experimental data. However, we found it useful to compare the results of Sawada *et al*'s 2D simulation for a single-spot contact carried out in [13] with those of our analytical model leading to Eq. (4b). The comparison is shown in Fig. 12 for the two film thicknesses for which Sawada *et al* [13] carried out their calculations. Very good agreement is noted, thus confirming the accuracy of our analytical calculations of spreading resistance for the model of Fig. 1. This may also be considered as a validation of the codes of Sawada *et al* [13] who also simulated a 3-dimensional geometry. We re-emphasize that the disagreement between theory (both Sawada *et al*'s and ours) and the experimental data in [13] probably stems from the use of too small a value of the bulk resistance in extracting spreading resistance from the measured total resistance values.

VI. Concluding Remarks

In this paper, we have summarized the results of numerical evaluations of constriction resistance shown in the geometry of Fig. 1, for both Cartesian and cylindrical thin films. The in-depth study of this relatively simple geometry has offered two new insights relating to constriction resistance: (i) the normalized spreading resistance does not tend to zero in the limit $h \rightarrow 0$ [Figs. 2, 3], and (ii) there is an intimate relation between contact resistance in a DC thin film and AC constriction resistance in a bulk solid at high signal frequencies [Fig. 8]. Significant extension of the model of Fig. 1 is given in [17], [18].

References

[1] W. J. Greig, *Integrated Circuit Packaging, Assembly and Interconnections*, Springer, New York, 2007.

[2] D. K. Schroder, *Semiconductor Material and Device Characterization*, 2 ed., Wiley & Sons, New York, 1998, p.149.

[3] R. Holm, *Electric Contact*, Springer-Verlag, Berlin, ed. 4, 1967; P. G. Slade, ed., *Electrical Contacts: Principles and Applications*, New York: Marcel Dekker, 1999.

[4] R. S. Timsit, "Electrical contact resistance: properties of stationary interfaces", IEEE Trans. Compon. Packag. Technol., vol. 22, p. 85, 1999.

[5] Y. H. Jang, J. R. Barber, and S. Jack Hu, "Electrical conductance between conductors with dissimilar temperature-dependent material properties", J. Phys. D: Appl. Phys., vol. 31, p. 3197, 1998.

[6] P. Zhang, Y. Y. Lau, and R. M. Gilgenbach, "Thin film contact resistance with dissimilar materials", J. Appl. Phys., vol. 109, p. 124910, 2011.

[7] P. Zhang, "Effects of Surface Roughness on Electrical Contact, RF Heating and Field Enhancement", doctoral dissertation, University of Michigan, Ann Arbor (2012).

[8] P. Zhang, Y. Y. Lau, and R. S. Timsit, "On the Spreading Resistance of Thin-Film Contacts", IEEE Trans. Electron Devices, vol. 59, p. 1936, 2012.

[9] R. Timsit, "Constriction resistance of thin-film contacts," IEEE Trans. Compon. Packag. Technol., vol. 33, p. 636, 2010.

[10] J. D. Lavers and R. Timsit, "Constriction resistance at high signal frequencies", IEEE Trans. Compon. Packag. Technol., vol. 25, p. 446, 2002.

[11] M.B. Read, J.H. Lang, A.H. Slocum and R. Martens, "Contact resistance in flat thin films", Proc. 55th IEEE Holm Conf. Electrical Contacts, p. 300, 2009.

[12] P. M. Hall, "Resistance calculations for thin film patterns," Thin Solid Films, vol. 1, no. 4, p. 277, 1968.

[13] S. Sawada, S. Tsukiji, S. Shimada, T. Tamai and Y. Hattori, "Current Density Analysis of Thin Film Effect in Contact Area on LED Wafer", Proc. 58th IEEE Holm Conf. on Electrical Contacts, Portland, OR, 242 (2012).

[14] See http://www.ansoft.com for MAXWELL 2D software.

[15] J. A. Greenwood and J. B. P. Williamson, "Electrical conduction in solids. II. Theory of temperature-dependent conductors," Proc. R. Soc.A, vol. 246, no. 1244, pp. 13–31, Jul. 1958.

[16] S. Sawada, private communication, Feb 2013.

[17] P. Zhang, D. Hung, and Y. Y. Lau, "Current flow in a 3-terminal thin film contact with dissimilar materials and general geometric aspect ratios", J. Phys. D: Appl. Phys., vol. 46, p. 065502, 2013; Corrigendum, ibid, vol. 46, p. 209501, 2013.

[18] P. Zhang and Y. Y. Lau, "Constriction resistance and current crowding in vertical thin film contact," IEEE J. Electron Dev. Soc., in the press, 2013.